Designing high electron mobility transistor heterostructures with quantum dots for efficient, number-resolving photon detection

M. A. Rowe, E. J. Gansen, and M. B. Greene
Optoelectronics Division, National Institute of Standards and Technology, Boulder, Colorado 80305

D. Rosenberg
Los Alamos National Laboratory, Los Alamos, New Mexico 87545

T. E. Harvey and M. Y. Su
Optoelectronics Division, National Institute of Standards and Technology, Boulder, Colorado 80305

R. H. Hadfield
Heriot-Watt University, Edinburgh E 14 4AS, United Kingdom

S. W. Nam and R. P. Mirin[a)]
Optoelectronics Division, National Institute of Standards and Technology, Boulder, Colorado 80305

(Received 26 October 2007; accepted 30 December 2007; published 30 May 2008)

We describe the design of the epitaxial layers for an efficient, photon-number-determining detector that utilizes a layer of self-assembled quantum dots as an optically addressable gate in a field-effect transistor. Our design features a dedicated absorption layer where photoexcited holes are produced and directed with tailored electric fields to the quantum dot layer. A barrier layer ensures that the quantum dot layer is located at a two-dimensional potential minimum of the structure for the efficient collection of holes. Using quantum dots as charge traps allows us to contain the photoexcited holes in a well-defined plane. We derive an equation for a uniform size of the photon signal based on this precise geometry. Finally, we show corroborating data with well-resolved signals corresponding to different numbers of photons. © *2008 American Vacuum Society.* [DOI: 10.1116/1.2837839]

Self-assembled quantum dots (QDs) can be controllably positioned in semiconductor heterostructures and provide stable, three-dimensional confinement of charge. These attributes have prompted a number of investigations into the suitability of QD heterostructures as optically addressable memories[1–6] and sensitive detectors.[7] In the case of optical memories, carriers excited by an optical write pulse are stored in QDs, resulting in a long-lived memory. Both electrical and optical charge-state readouts have been demonstrated. Electrical readout is accomplished by embedding the QDs in a field-effect transistor (FET) and using a two-dimensional electron gas (2DEG) to monitor the charge stored in the dots (so-called persistent photoconductivity). Although such devices are often presented as optically addressable memories, they effectively function as photodetectors as well. In fact, it has been shown that for sufficiently small active areas, FET structures can sense the change in the 2DEG current caused by the absorption of even a single photon of light.[7–9] In order to implement this type of single-photon detector in practical applications, high detection efficiency is desirable. In addition, certain applications require detectors that are not only sensitive to single photons but that can also directly measure the photon-number state of a pulse of light. This ability of detectors to discriminate between different numbers of photons is important in quantum optics[10] and in the quantum information field where applications include quantum cryptography[11] and computing.[12]

Here, we describe the epitaxial design for a quantum dot, optically gated, field-effect transistor (QDOGFET) photodetector,[9,13–15] where we specifically design the epitaxial layers for efficient, single-shot, photon-number-resolving detection.

The detector material is grown on a GaAs substrate using molecular beam epitaxy. Figure 1 shows the heterostructure layers. The semiconductor heterostructure (from bottom to top) consists of a 200 nm GaAs buffer layer, a 2.5 μm $Al_{0.20}Ga_{0.80}As$ layer, Si δ doping ($\sim 1 \times 10^{12}$ cm^{-2}), a 70 nm $Al_{0.20}Ga_{0.80}As$ layer, a 100 nm GaAs absorption layer, InGaAs self-assembled QDs (400–500 μm^{-2}), a 200 nm $Al_{0.20}Ga_{0.80}As$ barrier layer, and a 10 nm n-doped ($\sim 6 \times 10^{17}$ cm^{-3}) GaAs cap layer. Because the interior $Al_{0.20}Ga_{0.80}As$ layer contains δ doping, a 2DEG forms at the edge of the GaAs absorption layer opposite the QDs. The interior $Al_{0.20}Ga_{0.80}As$ layer is grown quite thick in order to minimize contributions from the secondary 2DEG at the buffer layer/heterojunction layer interface.[15] Contact is made to the primary 2DEG by depositing and annealing Ni/Au/Ge source and drain contacts. A channel mesa is subsequently etched between the source/drain contacts and a semitransparent Pt Schottky barrier gate is deposited midchannel. A scanning electron microscope (SEM) image of a completed device is shown in Fig. 2. The active area of the detector is located where the gate and the channel intersect. For single-photon sensitive devices, the active area is typically a few square micrometers. The devices have an opaque Au mask

[a)]Electronic mail: mirin@boulder.nist.gov

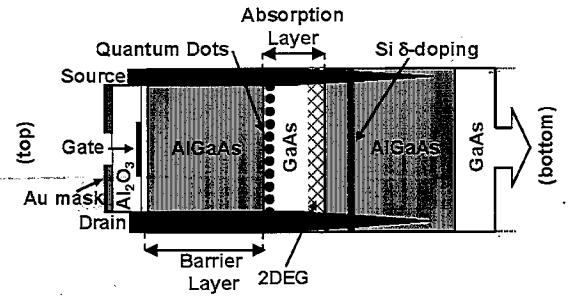

FIG. 1. Schematic diagram of the QDOGFET showing the heterostructure layers and the device fabrication.

that covers the edges of the active area, leaving the interior of the active area uncovered.

The heterostructure contains a dedicated absorption layer that is designed to efficiently detect absorbed photons. As illustrated in Fig. 3, the detection dynamics take place in this layer. Photoexcited charge must only be efficiently directed to the QDs from this dedicated layer, simplifying design considerations. Absorption is restricted to the absorption layer by exploiting the different band gaps of GaAs and $Al_{0.20}Ga_{0.80}As$. Photons with wavelengths ranging from about 700 to 815 nm (device at 4 K) are absorbed in the active GaAs layer and not in the AlGaAs layers of the structure. By illuminating the device within this optical bandwidth, the carrier transport involved with detection is isolated to the GaAs absorption layer. GaAs is a relatively defect-free absorption material, making it a good medium for transporting charge. By contrast, AlGaAs contains a high concentration of defects, which can trap carriers,[16] making it less than ideal. In fact, detectors have been demonstrated without QDs, where the photoexcited charge is stored only in DX^- centers and neutral donors.[8] This is not desirable for our detector because we want to control where the photoexcited charges are stored (in QDs) in order to obtain a uniform detector response. With its distinct absorption region, the dedicated absorption layer design can accommodate the addition of a multipass mechanism. For instance, the heterostructure could be embedded in a resonant cavity such that incoming light passes multiple times across the absorption layer without being absorbed elsewhere in the structure. This absorption layer concept could be extended to other wavelength ranges by using different materials. For example, an InGaAs/InAlAs/InP heterostructure utilizing InAs QDs could be used to extend this device into the 1550 nm telecommunications band, where even good single-photon detectors are not readily available.

In our device, the QD layer functions as an engineerable plane of deep charge traps. Photogenerated holes confined to the dots screen the gate field changing the conductance of the 2DEG. Our heterostructure geometry, with its fixed distance between the QDs and the 2DEG, results in uniform photoresponses, which we calculate below. This aspect of the device design is critical for achieving good photon-number resolution. To maximize the amplitude of the photoresponse and the quantum efficiency of the detection mechanism, it is important to separate the electrons and holes and to direct only

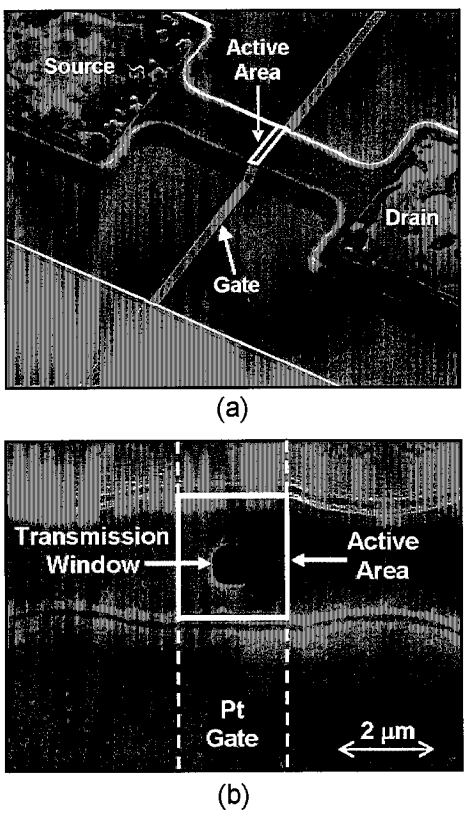

FIG. 2. Scanning electron microscope (SEM) images showing (a) a QDOGFET fabricated without an opaque Au mask and (b) a close-up of the active area of a QDOGFET fabricated with an opaque Au mask. The active areas are 0.7×3.9 μm^2, for (a) and 2.0×2.4 μm^2 for (b). The transmission window in (b) is 0.7×0.7 μm^2.

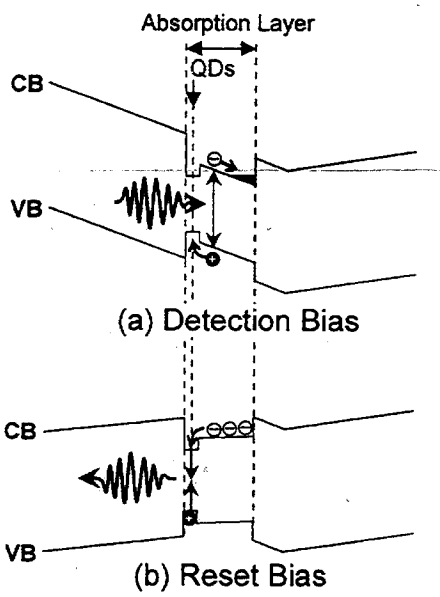

FIG. 3. Band diagrams for the QDOGFET heterostructure (a) under detection bias and (b) under reset bias. CB and VB denote the conduction and valence bands, respectively.

one charge polarity to the QDs. Spatially separating the electrons and holes minimizes recombination that would lead to missed photocounts, and maximizes the screening of the gate field. As shown in Fig. 3(a), such control of the photoexcited carriers is accomplished with our structural design. The gate field separates the electrons and holes excited throughout the absorption layer, directing the electrons toward the 2DEG and, concurrently, the holes toward the QDs. In order to efficiently capture the holes, we add an $Al_{0.20}Ga_{0.80}As$ barrier layer to the conventional inverted structure. The barrier layer is placed against the QD layer, where it blocks carriers from transporting past the QD layer. The holes move to the two-dimensional potential minimum located at the QD layer and then efficiently collect in the QDs.

Although the charge storage time of QDs can be quite long, our detector design allows for convenient electrical reset. Figure 3(b) shows the band diagram for the heterostructure with the reset bias, $\sim+1$ V applied to the gate. Under this bias, the electrons flow from the 2DEG to the QDs. Here, they radiatively recombine with the trapped holes, resetting the device. By studying the photoluminescence emitted from the QDs during reset, we have shown that the carriers recombine in less than a microsecond (resolution limited by detection electronics),[13] enabling high-speed operation.

In addition to functioning as an efficient photodetector, the FET also serves as an ultrasensitive, charge-sensitive amplifier. Its photoconductive gain makes the detector sensitive to the photoexcited charge from even a single photon. Figure 4 shows the conduction bands for the detector before [Fig. 4(a)] and after [Fig. 4(b)] the QDs are filled along with schematic representations of the corresponding uncharged and charged heterostructures. Illustrated in the figure are the three charged layers of the device—the gate, the QDs, and the channel—with a fixed bias, V_{gate}, applied between the gate and channel. The bias value is chosen such that the 2DEG is partially filled and is maximally sensitive to the screening by the trapped holes. When photons are absorbed, the resulting holes charge the QD layer of the device, as illustrated in Fig. 4(b). Responding to the charging of the QD layer, electrons redistribute themselves between the channel and the gate, in order to maintain the potential difference between the gate and channel. N trapped holes result in the addition of $N_{channel}$ electrons in the channel and N_{gate} electrons on the gate. Note that $N_{channel}+N_{gate}=N$. In order to keep the potential between the gate and channel constant,

$$N_{channel}=\frac{W}{D}N, \tag{1}$$

where W and D are the distances from the gate to the QDs and channel, respectively. The design trade-offs involved in choosing the layer thicknesses are illuminated with this W/D scaling. In order to maximize the fraction of the charge distributed to the channel $W\sim D$ is needed. However, to maximize the absorption length without burying the 2DEG too deeply $D\gg W$ is desired. We used a compromise value of $D/W=3/2$ with a 100 nm absorption layer. In this case, 10%

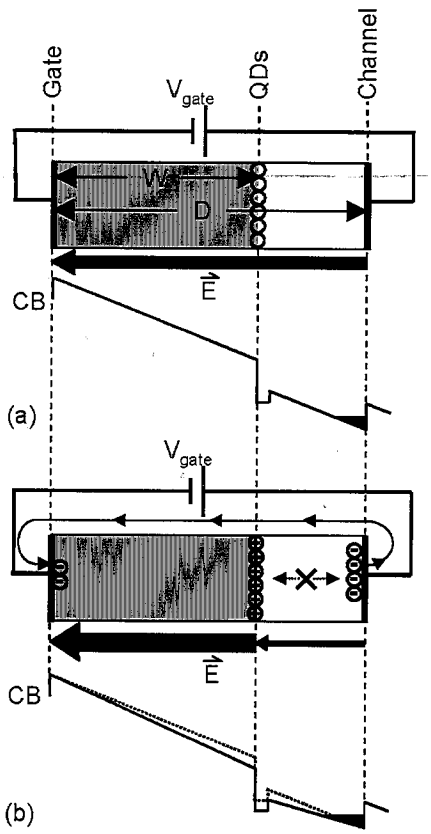

FIG. 4. Heterostructure charge distributions with a constant gate/channel bias, V_{gate}, and the corresponding conduction band (CB) diagrams for the QDOGFET (a) without filled QDs and (b) with filled QDs. The unscreened (a) and screened (b) electric fields are shown with the arrows labeled **E**. The X and arrows in (b) represent the creation of photoexcited carriers in the absorption layer and their distribution to the QDs, channel, and gate.

of the passing photons are absorbed in the absorption layer and the 2DEG is located 300 nm below the heterostructure surface.

Although the applied gate bias remains constant during illumination, the positively charged QDs screen the gate field effectively changing the gate voltage. As illustrated in Fig. 4(b), the confined holes pull the conduction band down in the vicinity of the QDs, which, in turn, increases the electron population of the 2DEG. The effective change in the gate voltage,[1] ΔV_{gate}, produced by the addition of N positive charges to the plane of the QDs is calculated from Eq. (1) and the gate/channel capacitance of the device ($C=\varepsilon' A/eD$) and is given by

$$\Delta V_{gate}=\frac{eW}{\varepsilon' A}N. \tag{2}$$

Here, e is the elementary charge, ε' is the electric permittivity of the material, and A is the active area of the detector. This is the voltage change necessary to alter the channel current (without charging the QDs) by the same amount as charging the QDs (with a constant gate bias). In the small signal limit, the channel current change, ΔI_{ds}, is simply related to ΔV_{gate} via the transconductance g_m of the FET.

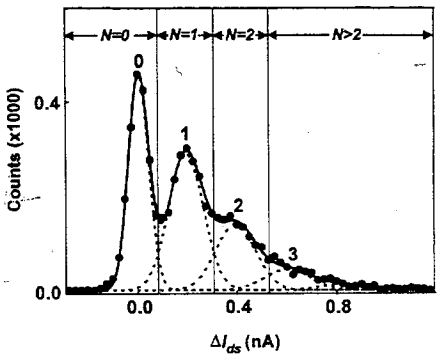

FIG. 5. Histogram of binned current changes, ΔI_{ds} for a mean number of detected photons, $\bar{N}=1.1$. The solid curve is a Poissonian fit to the data, where the detector response is taken into account by assuming a Gaussian distribution (dashed curves) for each labeled photon-number peak. The solid verical lines indicate the decision regions for determining $N=0$, 1, 2, or >2 for a specific laser pulse. The active area for the detector was 2.0 μm long by 2.4 μm wide. Photoabsorption was limited to the interior of the active area by an opaque Au mask with a 0.7×0.7 μm^2 transmission window.

$$\Delta I_{ds} = g_m \Delta V_{gate} = g_m \frac{eW}{\varepsilon' A} N. \tag{3}$$

The charging of even a single QD by a photogenerated hole results in a large change in the cumulative charge transferred in the channel. This photoconductive gain[17] gives the detector its single-photon sensitivity. Moreover, Eq. (3) predicts a uniform response to each photon that is additive so the size of the signal is a direct measure of the number of detected photons.

Recent measurements of the photoresponse of the QDOGFET to low fluxes of photons support our design considerations. In a first set of experiments,[9] we demonstrated the single-photon sensitivity of the detector and verified quantitatively the linear response predicted by Eq. (3). In addition, the efficiency considerations of the QDOGFET's design were verified by measuring the detector's internal quantum efficiency. We were careful to identify and subtract background counts not associated with the QDs. The resulting internal quantum efficiency, the fraction of the photons detected out of the number absorbed in the absorption layer, was indeed high, ~70%. In a next set of experiments,[14] we made improvements to reduce background signals and eliminate the diminutive signals from the edges of the active area. With these improvements, we demonstrated the photon-number resolving capabilities of the QDOGFET.

The QDOGFET's response to highly attenuated laser pulses via the channel current changes, ΔI_{ds}, were binned into histograms in order to show the well-defined peaks associated with the detection of discrete numbers of photons. Figure 5 shows one such histogram where the mean number of detected photons in each laser pulse, $\bar{N}$, was 1.1. The four Gaussian functions (shown as dashed curves in Fig. 5) account for the detection of $N=0$, 1, 2, and 3 photons. The solid curve is the sum of these four Gaussian functions. The areas of the Gaussians obey the Poissonian distribution for $\bar{N}=1.1$. The centers of the Gaussian functions are positioned at intervals of 0.20 ± 0.02 nA. In addition, the average current change produced by each detected photon as calculated by $\mu/\bar{N}$ (μ is the distribution mean) is 0.19 ± 0.01 nA, showing that the analysis is self-consistent. These obtained values for the single-photon signal are in good agreement with Eq. (3), which predict that the current change produced by each detected photon should be 0.19 nA. The different regions shown in Fig. 5 (marked $N=0$, $N=1$, $N=2$, and $N>2$) are decision regions for determining N for a given laser pulse. The probability of accurately determining N for a single shot is found by dividing the area of the primary Gaussian function contained within the corresponding decision region by the total area of all the Gaussian functions contained within that region. For this data with $\bar{N}=1.1$, we can determine N for each pulse with $\geqslant$83% confidence.

In summary, we have described the QDOGFET heterostructure, which was designed specifically for sensitive photon detection. The internal quantum efficiency of our device is ~70%. This high efficiency of the underlying dynamics should make the heterostructure suitable for developing a detector with high overall quantum detection efficiency. To achieve this goal, light must be efficiently coupled to the active area of the device and a transparent material used for the gate. In addition, incorporating the heterostructure layers in a resonant cavity should greatly increase the overall efficiency. The photon-number-resolving capabilities of the QDOGFET were measured and are consistent with the heterostructure model. For data with $\bar{N}=1.1$, different numbers of photons produced well-resolved signals for which the number state could be determined with $\geqslant$83% accuracy for a single laser pulse.

[1]G. Yusa and H. Sakaki, Electron. Lett. **32**, 491 (1996).
[2]G. Yusa and H. Sakaki, Appl. Phys. Lett. **70**, 345 (1997).
[3]J. J. Finley, M. Skalitz, M. Arzberger, A. Zrenner, G. Böhm, and G. Abstreiter, Appl. Phys. Lett. **73**, 2618 (1998).
[4]H. Pettersson, L. Baath, N. Carlsson, W. Seifert, and L. Samuelson, Appl. Phys. Lett. **79**, 78 (2001).
[5]M. Kroutvar, Y. Ducommun, J. J. Finley, M. Bichler, G. Abstreiter, and A. Zrenner, Appl. Phys. Lett. **83**, 443 (2003).
[6]T. Lundstrom, W. Schoenfeld, H. Lee, and P. M. Petroff, Science **286**, 2312 (1999).
[7]A. J. Shields, M. P. O'Sullivan, I. Farrer, D. A. Ritchie, K. Cooper, C. L. Foden, and M. Pepper, Appl. Phys. Lett. **74**, 735 (1999).
[8]H. Kosaka, D. S. Rao, H. D. Robinson, P. Bandaru, T. Sakamoto, and E. Yablonovitch, Phys. Rev. B **65**, 201307 (2002).
[9]M. A. Rowe *et al.*, Appl. Phys. Lett. **89**, 253505 (2006).
[10]L. Mandel and E. Wolf, *Optical Coherence and Quantum Optics* (Cambridge University Press, New York, 1995).
[11]C. H. Bennett, F. Bessette, G. Brassard, L. Salvail, and J. Smolin, J. Cryptology **5**, 3 (1992).
[12]E. Knill, R. Leflamme, and G. J. Milburn, Nature (London) **409**, 46 (2001).
[13]E. J. Gansen *et al.*, IEEE J. Sel. Top. Quantum Electron. **13**, 967 (2007).
[14]E. J. Gansen *et al.*, Nat. Photonics **1**, 585 (2007).
[15]E. J. Gansen *et al.*, Proc. SPIE **6771**, 67710Y-1 (2007).
[16]P. M. Mooney, J. Appl. Phys. **67**, 1 (1990).
[17]A. Rose, *Concepts in Photoconductivity and Allied Problems* (Interscience, New York, 1963), Chap. 1.